

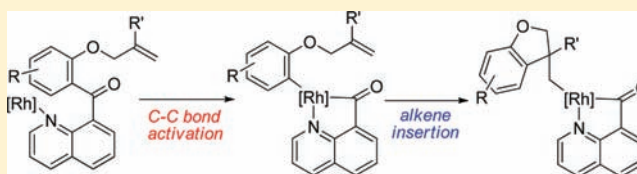
Rate-Limiting Step of the Rh-Catalyzed Carboacylation of Alkenes: C–C Bond Activation or Migratory Insertion?

J. Patrick Lutz, Colin M. Rathbun, Susan M. Stevenson, Breanna M. Powell, Timothy S. Boman, Casey E. Baxter, John M. Zona, and Jeffrey B. Johnson*

Department of Chemistry, Hope College, 35 East 12th Street, Holland, Michigan 49423, United States

S Supporting Information

ABSTRACT: Rhodium-catalyzed intramolecular carboacylation of alkenes, achieved using quinolinyl ketones containing tethered alkenes, proceeds via the activation and functionalization of a carbon–carbon single bond. This transformation has been demonstrated using $\text{RhCl}(\text{PPh}_3)_3$ and $[\text{Rh}(\text{C}_2\text{H}_4)_2\text{Cl}]_2$ catalysts. Mechanistic investigations of these systems, including determination of the rate law and kinetic isotope effects, were utilized to identify a change in mechanism with substrate. With each catalyst, the transformation occurs via rate-limiting carbon–carbon bond activation for species with minimal alkene substitution, but alkene insertion becomes rate-limiting for more sterically encumbered substrates. Hammett studies and analysis of a series of substituted analogues provide additional insight into the nature of these turnover-limiting elementary steps of catalysis and the relative energies of the carbon–carbon bond activation and alkene insertion steps.



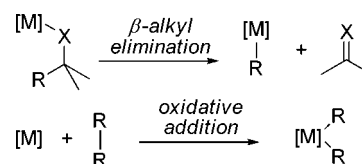
INTRODUCTION

Transition-metal catalysis has a continual influence on the evolution of synthetic organic chemistry.¹ Rarely is a new complex synthetic molecule completed without the use of a cross-coupling, an olefin metathesis, or another transition-metal-catalyzed reaction that was unknown as little as 30 years ago. A constant stream of new methods has led to innumerable synthetic possibilities with greater selectivity and efficiency.

Despite this stream of new methods and the battery of functional groups utilized for coupling, activation, and modification, the carbon–carbon single bond has remained virtually untouched and is typically considered to be an inert functionality.² Whereas even the nonpolar and highly inert C–H bond has slowly been assimilated into mainstream synthetic use as a functional group in transition-metal catalysis,³ efforts to trigger a similar development of carbon–carbon single bonds remain in relative infancy. Although limited rudimentary means to cleave these nonpolar and highly inert moieties have been available for many years, transition-metal-catalyzed methods for the cleavage of carbon–carbon bonds remain relatively rare.^{4,5} Existing methods generally rely on substrate-specific strategies such as substrates with formation of highly stabilized carbanions,^{6–8} ring strain,⁹ or enforced proximity^{10,11} to induce C–C bond cleavage.

The majority of transition-metal-catalyzed carbon–carbon single bond activation reactions are believed to proceed through one of two general mechanisms: β -alkyl elimination and oxidative addition (Scheme 1). Although both mechanisms generate an organometallic intermediate, the nature of these species can vary significantly. The oxidative addition mechanism leads to an organometallic species with two metal–alkyl fragments, whereas the β -alkyl elimination mechanism leads to

Scheme 1



a metal center with a single alkyl group. This distinction has a significant influence on what functionalization processes can follow the activation step.

As the number of methods for transition-metal-catalyzed carbon–carbon bond activation slowly increases, the emphasis has shifted beyond simple single bond cleavage toward functionalization of the organic fragments. This has been accomplished in a number of ways, the most simple of which are hydrogenation, protonolysis, or rearrangement via β -alkyl elimination.¹² Other reactions, particularly those proceeding via β -alkyl elimination, have achieved cross-coupling with aryl halides^{13,14} or addition to carbonyls,^{15,16} alkenes,¹⁷ or Michael acceptors.¹⁸ For reactions proceeding through an oxidative addition mechanism, several functionalization routes are possible, but the most powerful methodology is that in which two organometallic fragments can be added across a π bond in an alkyne or alkene.¹⁹ This transformation results in two new carbon–carbon bonds, and when utilized with alkenes,^{20,21} this reaction holds the potential to generate two stereocenters.²² The overall process, formally the insertion of an alkene into a carbon–carbon single bond, represents a reaction with a

Received: November 2, 2011

Published: December 1, 2011

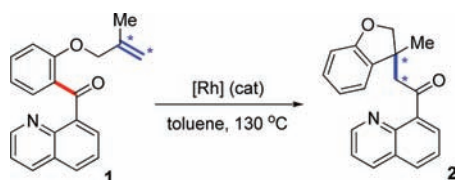
tremendous potential for a rapid increase in molecular complexity.

Although reactions utilizing carbon–carbon activation and functionalization sequences remain largely undeveloped, these transition-metal-catalyzed processes have the potential to follow the trajectory of C–H activation methodology, developing from an esoteric area of study to a battery of reactions that offer a wide range of previously unrealized retrosynthetic disconnects. Our contribution to the development of new methodologies utilizing carbon–carbon single bond activation focuses on the increased understanding of the factors that guide this relatively unknown process.²³ To date, mechanistic studies of transition-metal-catalyzed carbon–carbon bond activation processes are quite sparse, limited primarily to reactions utilizing strained substrates and the activation of carbon–nitride bonds.^{24,25} Additional insight into the nature of the transition-metal-catalyzed activation of carbon–carbon single bonds promises to benefit the development of future reactions. As the factors that influence carbon–carbon bond cleavage become more clear, this information can be utilized to generate new methods to further enhance the general area of carbon–carbon activation and lead to new reactions and methodology amenable to the synthesis and manipulation of complex molecules.

BACKGROUND

To gain additional understanding of the process of carbon–carbon single bond activation, our group initiated the mechanistic investigation of the intramolecular carboacylation of alkenes achieved using quinolinyl ketones. This system, first reported by Douglas and co-workers,²⁰ represents a seminal example of the combination of a difficult carbon–carbon bond activation step with a subsequent reaction that significantly increases molecular complexity while simultaneously achieving this unique transformation in high efficiency (typically >90% yield) using rhodium catalysis with loadings down to 5 mol % (Scheme 2). The clean conversion observed with a majority of

Scheme 2



substrates makes this system an excellent focus of a mechanistic study. In previously communicated work, our group performed a kinetic analysis of this system and identified that utilizing Wilkinson's catalyst, carbon–carbon bond activation serves as the turnover-limiting step of catalysis.²³ Herein we describe additional studies that significantly increase our understanding of the mechanism of the $\text{RhCl}(\text{PPh}_3)_3$ -catalyzed reaction and also provide an analysis of the reaction performed under $[\text{Rh}(\text{C}_2\text{H}_4)_2\text{Cl}]_2$ catalysis, which demonstrates a notably different kinetic profile. These results are combined to generate significant insight into the general process of transition-metal-catalyzed carbon–carbon bond activation.

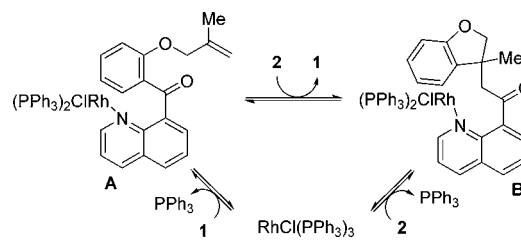
As previously reported, the carboacylation of quinolinyl ketone **1** catalyzed by Wilkinson's catalyst was examined using traditional kinetic methods as well as through the use of $^{12}\text{C}/^{13}\text{C}$ kinetic isotope effects.²³ The kinetic analysis revealed a

rate law in which the reaction demonstrates zero-order dependence on substrate concentration and first-order dependence on catalyst concentration (eq 1). The combined results yielded an overall first-order rate law with a rate constant of $k = 4.98 \times 10^{-4} \text{ s}^{-1}$ at 130 °C.

$$-\frac{d[\mathbf{1}]}{dt} = k[\text{Rh}]^1[\mathbf{1}]^0 \quad (1)$$

The observation of a rate law with a zero-order substrate dependence was rationalized by proposing substrate–rhodium complex **A** as the resting state of catalysis (Scheme 3).

Scheme 3



Additional studies identified the occurrence of product inhibition, but only at high excess concentrations of product **2** relative to substrate **1**. Thus, under typical reaction conditions, complex **A** is the resting state. Significant conversion of the starting material results in sufficient concentrations of **2** to competitively bind to the metal center, shifting the resting state to a mixture between **A** and **B**, resulting in a marked decrease of the reaction rate as the reaction nears completion.

Additional kinetic experiments revealed the inhibitory effect of exogenous PPh_3 on the reaction rate. The presence of additional PPh_3 presumably shifts the equilibrium of the resting state from the Rh–quinolinyl ketone complex back toward $\text{RhCl}(\text{PPh}_3)_3$, thus slowing the reaction.

As the carboacylation is an intramolecular reaction, it is impossible to probe the relative energies of the proposed C–C bond activation (oxidative addition), migratory insertion of the alkene, and reductive elimination steps through traditional kinetic methods. An alternative method, determination of the $^{12}\text{C}/^{13}\text{C}$ kinetic isotope effects, was utilized to gain additional insight into the nature of the turnover-limiting step. Following the protocol developed by Singleton,²⁶ isotope effects were determined for a number of carbons, with the results summarized in Figure 1. Statistically significant kinetic isotope

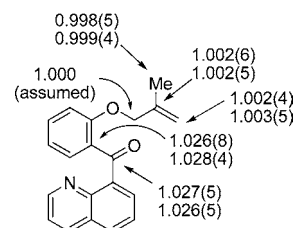
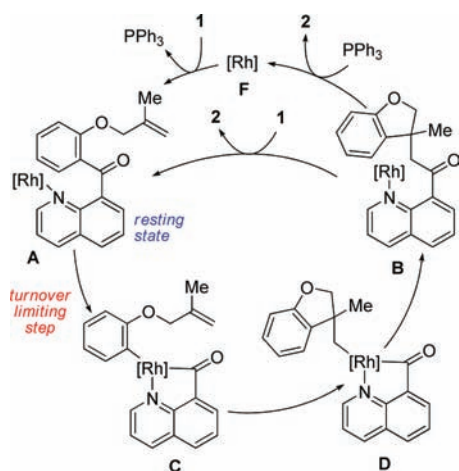


Figure 1. Observed $^{12}\text{C}/^{13}\text{C}$ kinetic isotope effects for select carbons during the $\text{RhCl}(\text{PPh}_3)_3$ -catalyzed carboacylation of **1**.

effects were observed at the ketone carbon (1.027 ± 0.005 and 1.026 ± 0.005) and the adjacent aromatic carbon (1.026 ± 0.008 and 1.028 ± 0.004). In contrast, the isotope effects observed on the alkene carbons (all less than 1.003 and within error of 1.000) were negligible. These results suggest that the ketone–aryl bond is

involved in the turnover-limiting step of catalysis, while there is no involvement of the alkene. The observation of significant kinetic isotope effects on both the ketone and aryl carbons provides support for an oxidative addition-type activation of the carbon–carbon single bond, leading to rhodium–acyl–arene intermediate C. A complete view of the catalytic cycle is provided in Scheme 4.

Scheme 4. Proposed Catalytic Cycle under $\text{RhCl}(\text{PPh}_3)_3$ Catalysis



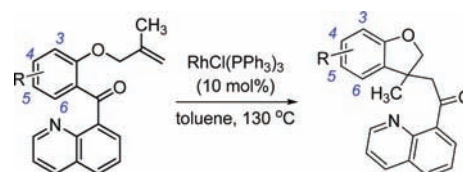
Following identification of the resting state and turnover-limiting step of catalysis, the reaction was run at temperatures between 110 and 140 °C to determine the activation enthalpy ($\Delta H^\ddagger = 27.8 \pm 1.0$ kcal/mol) and the activation entropy ($\Delta S^\ddagger = -4.3 \pm 2.4$ eu). The near-neutral value obtained for the activation entropy is consistent with the hypothesis of a rhodium–quinoline complex as the resting state and carbon–carbon bond activation as the turnover-limiting step. These results also provide a quantitative value for the energy required to cleave the carbon–carbon single bond within the context of a transition-metal-catalyzed system.

RESULTS

Aromatic Substitution. To obtain additional information on the nature of the transition state required for the cleavage of the carbon–carbon single bond under $\text{RhCl}(\text{PPh}_3)_3$ catalysis, we prepared a series of analogues of the parent quinolinyl ketone **1**. Three areas of substitution were examined: on the alkene, on the quinoline, and on the bridging aryl group. Several species containing alkene substitution have been previously reported, while those with substitution upon the quinoline and the aryl group were prepared in analogy to the literature procedure.²⁰ Aryl substitution provided the largest range of species, including those with either electron-donating or electron-withdrawing functionality as well as those with significant steric influence. Upon preparation, each species was subjected to carboacylation conditions using Wilkinson's catalyst (10 mol %) in toluene at 130 °C in a sealed tube. With the exception of sterically encumbered *tert*-butyl-substituted species **15**, each substrate was efficiently converted to the corresponding heterocycle and isolated in 85–97% yield, demonstrating a notable functional group tolerance that includes ethers, amines, alkyl halides, and nitro groups (Table 1).

Linear Free Energy Correlation. For each successful substrate containing aryl substitution, the reaction was performed in toluene- d_8 and the rate monitored by ^1H NMR

Table 1. $\text{RhCl}(\text{PPh}_3)_3$ -Catalyzed Carboacylation of Quinolinyl Ketones Containing Aryl Substitution



entry ^a	R, substrate	product	yield (%) ^b	k ($\text{s}^{-1} \times 10^4$) ^c
1	H, 1	2	97	4.98
2	3-OMe, 3	4	95	4.14
3	4-OMe, 5	6	93	8.35
4	5-OMe, 7	8	97	5.13
5	4-NEt ₂ , 9	10	85	12.5
6	5-NO ₂ , 11	12	91	2.32
7	5-Cl, 13	14	94	3.77
8	3,5-(<i>t</i> Bu) ₂ , 15	16	0	n/a

^aReaction conditions: 0.1 M substrate, 10 mol % $\text{RhCl}(\text{PPh}_3)_3$ in toluene at 130 °C. ^bIsolated yields. ^cThe average of three independent kinetic runs in toluene- d_8 .

to at least 80% conversion. Reaction with each compound was run using $\text{RhCl}(\text{PPh}_3)_3$ concentrations between 5.0 and 6.1 mM and between 0.08 and 0.11 M of substrate at 130 °C, and the rate constant was determined by fitting the data to a linear zero-order decay.²⁷ Each substrate reaction was run in triplicate, and the rate constant for each substrate was used to construct the Hammett plot provided in Figure 2. The σ values

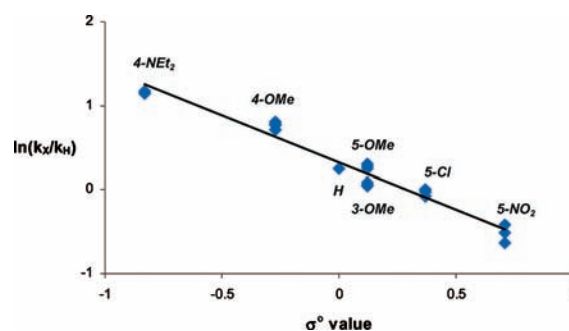
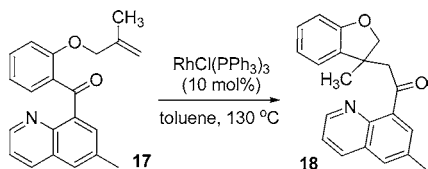


Figure 2. Linear free energy plot for the carboacylation of substituted quinolinyl ketones catalyzed by $\text{RhCl}(\text{PPh}_3)_3$ in toluene- d_8 at 130 °C.

represent the influence of the each substituent on the aryl–ketone bond that is cleaved in the reaction, and thus are designated as ortho, meta, or para relative to the ketone.²⁸ The resulting ρ value of -1.1 indicates that substrates containing substituents that donate electron density to the aryl–ketone bond undergo more rapid carbon–carbon bond activation than those that withdraw electron density.

Quinoline and Alkene Substitution. Several compounds containing quinolinyl or alkene substitution were also prepared and examined for reactivity in a manner similar to that described for the aryl-substituted compounds, using Wilkinson's catalyst. Methyl substitution upon the quinolinyl ring had no effect on carboacylation, producing the compound in 93% yield (Scheme 5). In contrast, however, substrates with any alteration on the pendant alkene, including the use of unsubstituted allyl, compounds with longer tethers, or 1,2-disubstituted alkenes, failed to produce the desired product under standard reaction conditions. The primary material recovered from these

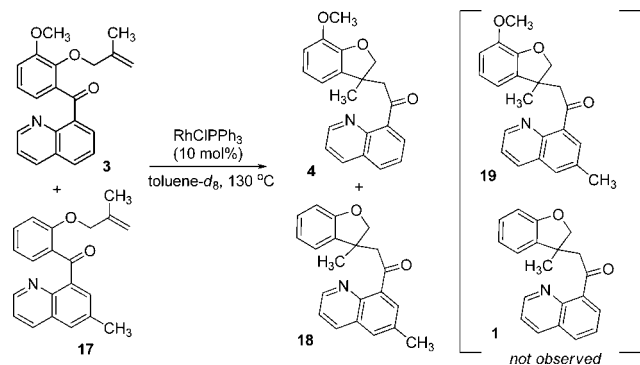
Scheme 5



unsuccessful reactions was unreacted starting material; at sufficiently long reaction times, decomposition of the starting material, apparently via cleavage of the allyl ether, was observed.

Crossover Experiment. To further probe the nature of the intermediates within the catalytic cycle and to assess the potential of bimetallic phenomenon, a crossover experiment was performed with 3-OMe-aryl-substituted substrate **3** and methyl-quinolinyl substrate **17** both present. Under $\text{RhCl}(\text{PPh}_3)_3$ catalysis, both substrates underwent full conversion to their corresponding products with no evidence of a mixing of molecular fragments, which would be illustrated by the observation of the unsubstituted parent product **1** or species **19**, which contains both OMe and Me substitution (Scheme 6).

Scheme 6



The results from this study suggest that rhodium–alkyl species are sufficiently short-lived to preclude intermolecular exchange during catalysis.

■ INVESTIGATION OF $[\text{Rh}(\text{C}_2\text{H}_4)_2\text{Cl}]_2$ Catalysis

As demonstrated by Douglas and co-workers, alternative catalysts, such as $[\text{Rh}(\text{C}_2\text{H}_4)_2\text{Cl}]_2$, can demonstrate differences in reactivity, most notably with substrates containing alkene substitution that fail to react using Wilkinson's catalyst.²⁰ To explore the differences, we initiated a second mechanistic investigation.

Rate Law. Our efforts began with a kinetic investigation of the parent compound, quinolinyl ketone **1**, using catalytic $[\text{Rh}(\text{C}_2\text{H}_4)_2\text{Cl}]_2$ in toluene- d_8 at 130 °C, and ^1H NMR spectroscopy was utilized to monitor the conversion of starting material. Using 0.00466 M $[\text{Rh}(\text{C}_2\text{H}_4)_2\text{Cl}]_2$, differences immediately became apparent, as the rate demonstrated a first-order dependence on the concentration of ketone **1** through at least 80% conversion at all initial substrate concentrations tested (0.12–0.16 M). Variation of the catalyst concentration between 2.3 and 9.3 mM revealed a first-order rate dependence on rhodium, thus leading to an overall second-order rate law (eq 2) in which $k = 0.0759 \text{ M}^{-1} \text{ s}^{-1}$. This rate law is in contrast to that observed under $\text{RhCl}(\text{PPh}_3)_3$ catalysis, which demonstrates an overall first-order rate law with zero-order

dependence on the concentration of starting material.

$$-\frac{d[\mathbf{1}]}{dt} = k[\text{Rh}]^1[\mathbf{1}]^1 \quad (2)$$

To further probe the nature of the first-order dependence on starting material and discern whether this effect is due to product inhibition, two kinetic experiments were prepared under identical concentrations of catalyst (0.0036 M) and substrate (0.061 M), differing only by the presence of 0.146 M of product **2**. When these experiments were run side by side, no statistically significant rate difference was observed, indicating that the reaction rate is not inhibited by the presence of product.

$^{12}\text{C}/^{13}\text{C}$ Kinetic Isotope Effects. In order to identify the turnover-limiting step within what can be described as an isomerization reaction, the $^{12}\text{C}/^{13}\text{C}$ kinetic isotope effects were determined for the $[\text{Rh}(\text{C}_2\text{H}_4)_2\text{Cl}]_2$ -catalyzed carboacylation of parent compound **1**. In two reactions run on a gram scale to at least 85% conversion, reisolated starting material was subjected to quantitative ^{13}C NMR spectroscopy to determine the ^{13}C content. The $^{12}\text{C}/^{13}\text{C}$ kinetic isotope effects for the carbons potentially involved in the turnover-limiting step were determined and are provided in Figure 3.²⁹ Over two experiments, statistically

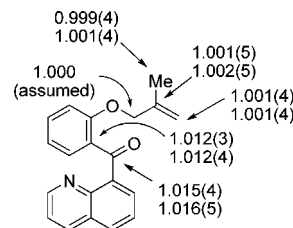
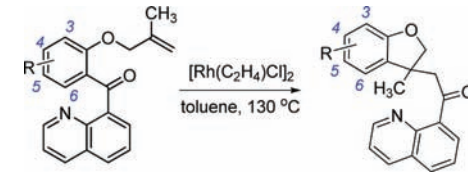


Figure 3. Observed $^{12}\text{C}/^{13}\text{C}$ kinetic isotope effects for select carbons during the $[\text{Rh}(\text{C}_2\text{H}_4)_2\text{Cl}]_2$ -catalyzed carboacylation of **1**.

significant isotope effects were determined for the ketone carbon (1.015 ± 0.004 and 1.016 ± 0.005) and the adjacent aromatic carbon (1.012 ± 0.003 and 1.012 ± 0.004). In contrast, negligible isotope effects (1.002 or less) were observed for the alkene carbons. These results clearly indicate turnover-limiting carbon–carbon bond activation.

Activation Parameters. Upon determination of the rate law for the carboacylation of **1**, further information was gathered by monitoring the rate of reaction at temperatures between 112 and 135 °C. Rate constants resulting from these kinetic runs were utilized to provide the activation parameters, $\Delta H^\ddagger = 28.4 \pm 1.3 \text{ kcal/mol}$ and $\Delta S^\ddagger = -26.4 \pm 2.6 \text{ eu}$, which describe the energy required for the cleavage of the carbon–carbon bond from the free rhodium resting state. The sizable negative entropy of activation suggests an associative process prior to the turnover-limiting step of catalysis.

Aromatic Substitution. To provide further insight into the mechanism of this transformation, the reaction rate was determined for a series of substituted analogues. Each compound was independently submitted to the standard reaction conditions (0.1 M substrate, 0.05 M $[\text{Rh}(\text{C}_2\text{H}_4)_2\text{Cl}]_2$ in toluene- d_8 at 130 °C) and monitored by ^1H NMR spectroscopy (Table 2). The conversion of each species was followed through at least 80% conversion, and in all cases followed first-order kinetics relative to the quinolinyl ketone. A linear free energy correlation of these values results in a ρ value of -0.4 (Figure 4).

Table 2. Screen of Quinoliny Ketones with Aryl Substitution for Carboacylation Using $[\text{Rh}(\text{C}_2\text{H}_4)_2\text{Cl}]_2$


entry ^a	R, substrate	product	yield (%) ^b	k ($\times 10^2 \text{ M}^{-1} \text{ s}^{-1}$) ^c
1	H, 1	2	96	7.59
2	3-OMe, 3	4	91	7.11
3	4-OMe, 5	6	87	9.69
4	4-NEt ₂ , 9	10	93	11.4
5	5-NO ₂ , 11	12	89	6.39
6	5-Cl, 13	14	94	6.72

^aReaction conditions: 0.1 M substrate, 10 mol % $[\text{Rh}(\text{C}_2\text{H}_4)_2\text{Cl}]_2$ in toluene at 130 °C. ^bIsolated yields. ^cThe average of three independent kinetic runs in toluene-*d*₈.

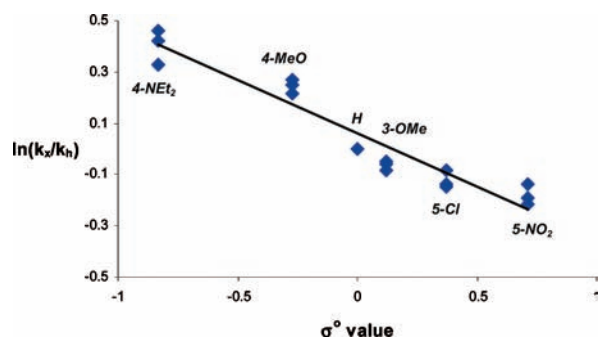


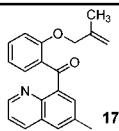
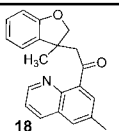
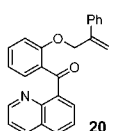
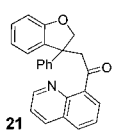
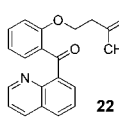
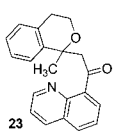
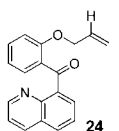
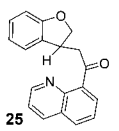
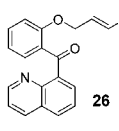
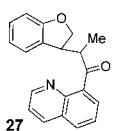
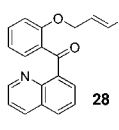
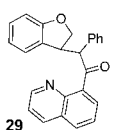
Figure 4. Linear free energy plot for the carboacylation of substituted quinoliny ketones catalyzed by $[\text{Rh}(\text{C}_2\text{H}_4)_2\text{Cl}]_2$ in toluene-*d*₈ at 130 °C.

Quinoline and Alkene Substitution. Our investigation continued with the examination of the reactivity of alkene-substituted analogues of the parent quinoliny ketone, including compounds 20, 22, and 24 previously described by Douglas and co-workers.^{20a} The results of this screen are provided in Table 3. As anticipated, the compounds with alkene substitution underwent successful carboacylation, as did those with aryl and quinoliny substitution. More insightful observations were obtained upon determining the rate constants for each of these alkene-substituted species. These compounds underwent reaction with significantly different rates relative to the parent ketone. Relative to the rate constant determined for the parent quinoliny ketone 1 ($k = 0.0759 \text{ M}^{-1} \text{ s}^{-1}$), replacement of the alkene methyl substitution with a phenyl group (20) resulted in a marked decrease in the reaction rate (Table 3, entry 2). Likewise, the use of quinoliny ketone 22 with its longer tether (entry 3) resulted in a further decrease in the rate of reaction. The compound with simple allyl substitution failed to produce the desired product (entry 4), presumably due to decomposition routes such as β -hydride elimination. It should also be noted that the attempted conversion of 1,2-disubstituted alkenes led to substrate decomposition with no formation of the desired product.

DISCUSSION

Methodology for selective carbon–carbon single bond activation and functionalization has vast potential, yet few methods have been developed to achieve such a transformation. In accordance with this scarcity, very little is known about the

Table 3. $[\text{Rh}(\text{C}_2\text{H}_4)_2\text{Cl}]_2$ -Catalyzed Carboacylation Utilizing Substrates with Quinoliny or Alkene Substitution

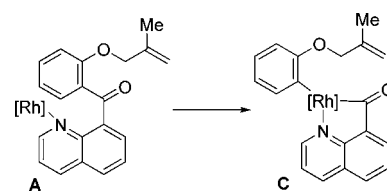
Entry ^a	Substrate, R	Product	Yield (%) ^b	k ($\text{M}^{-1} \text{ s}^{-1}$) ($\times 10^2$) ^c
1			94	7.90
2			91	2.62
3			89	1.20
4			17	n/a
5 ^d			<5	n/a
6 ^e			<5	n/a

^aReaction conditions: 0.1 M substrate, 10 mol % $[\text{Rh}(\text{C}_2\text{H}_4)_2\text{Cl}]_2$ in toluene at 130 °C. ^bIsolated yields. ^cThe average of three independent kinetic runs in toluene-*d*₈. ^dStarting material was a 85:15 mixture of trans:cis alkene isomers. ^eStarting material was a 3:1 mixture of trans:cis alkene isomers.

processes through which these reactions operate. This mechanistic investigation of the highly efficient rhodium-catalyzed intramolecular carboacylation of quinoliny ketones provides valuable insight into the mechanistic underpinnings of this transformation and the more general process of carbon–carbon bond activation.

Carboacylation under $\text{RhCl}(\text{PPh}_3)_3$ Catalysis. As previously described, the mechanism of $\text{RhCl}(\text{PPh}_3)_3$ -catalyzed alkene carboacylation has been determined to proceed via rate-limiting carbon–carbon single bond activation from rhodium–quinoliny ketone resting state A (Scheme 7).²³ From the linear

Scheme 7



free energy plot constructed with a series of substituted analogues of the parent quinoliny ketone, it was observed that the reaction rate correlated with the degree of electron

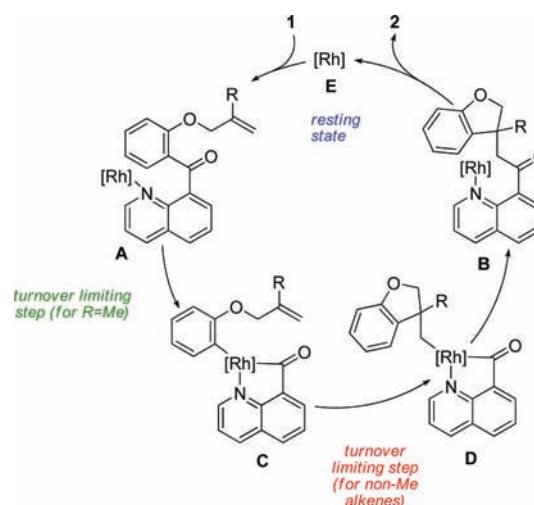
donation to the aromatic carbon–ketone bond. Substitution with the strongly electron-donating diethylamino substituent led to carboacylation that was 2.5 times more rapid than with the parent compound, while substitution with an electron-withdrawing nitro group reduced the rate by a factor of 2 relative to the parent compound. Although electron-donating substituents would be expected to strengthen the carbon–carbon bond destined for activation, the greater effect most likely comes through stabilization of the resulting intermediate, rhodium–alkyl intermediate C (Scheme 7). This intermediate, in the Rh(III) oxidation state, would presumably be more stable with more electron-rich substituents. The stability of this intermediate results in stabilization of the preceding transition state, thus leading to more rapid cleavage of the carbon–carbon single bond.

Carboacylation under $[\text{Rh}(\text{C}_2\text{H}_4)_2\text{Cl}]_2$ Catalysis. Based on observed differences in the reactivity of substrates utilizing $\text{RhCl}(\text{PPh}_3)_3$ versus $[\text{Rh}(\text{C}_2\text{H}_4)_2\text{Cl}]_2$, a mechanistic study was initiated to ascertain whether different mechanisms are operative within these catalytic cycles. Experiments immediately highlighted a difference in the kinetic nature of each reaction, as $[\text{Rh}(\text{C}_2\text{H}_4)_2\text{Cl}]_2$ catalysis results in an overall second-order rate law versus the first-order rate law determined using Wilkinson's catalyst. The first-order dependence of the rate on substrate concentration indicates that the substrate must be incorporated on the pathway from catalytic resting state to the turnover-limiting step. Furthermore, the absence of product inhibition suggests that the product does not remain bound to the catalyst to any appreciable degree. The combination of these observations suggests that the catalytic resting state is a rhodium catalyst unbound to substrate or product.

$^{12}\text{C}/^{13}\text{C}$ Kinetic Isotope Effects. Although the resting state has been identified, the rate law alone cannot distinguish the turnover-limiting step of catalysis in this intramolecular reaction. Any of three proposed elementary transformations—oxidative addition, alkene migratory insertion, and reductive elimination—could theoretically limit the reaction rate. Based on the breadth of data regarding the rate of reductive elimination from aryl–metal–alkyl species at far lower temperatures than utilized in this methodology, it is assumed that reductive elimination to form a $\text{C}_{\text{sp}^3}\text{--}\text{C}_{\text{sp}^2}$ bond is fast relative to other steps.^{30,31} The observation of $^{12}\text{C}/^{13}\text{C}$ kinetic isotope effects at the ketone and adjacent aromatic carbon, in addition to the lack of isotope effects on the alkene carbons, clearly indicates that under $[\text{Rh}(\text{C}_2\text{H}_4)_2\text{Cl}]_2$ catalysis, the rate of carboacylation of parent substrate 1 is limited by carbon–carbon bond activation. Compilation of the mechanistic information led to the catalytic cycle provided in Scheme 8.

Aromatic Substitution. Incorporation of electron-rich and electron-deficient substitution upon the aryl group of the quinolinyl ketone substrate influences the reaction rate in such a way that electron-rich substituents accelerate the reaction ($\rho = -0.4$). The rate of carboacylation was fastest with the most electron-rich diethylamino substituent (50% faster than the parent), while the use of a nitro-substituted aromatic ring led to a reaction rate approximately 75% that of the parent. This effect is similar to that observed under $\text{RhCl}(\text{PPh}_3)_3$ catalysis. With these substrates, catalyst turnover is limited by activation of the carbon–carbon bond; thus, the acceleration is attributed to the stabilization of the rhodium(III) acyl aromatic intermediate C generated upon activation of the carbon–carbon bond.

Scheme 8. Proposed Catalytic Cycle under $[\text{Rh}(\text{C}_2\text{H}_4)_2\text{Cl}]_2$ Catalysis



Alkene Substitution. Examination of substrates containing alkene substitution led to a markedly different mechanistic conclusion. Assuming that carbon–carbon bond activation limits catalyst turnover, it was expected that substrate alkene substitution would have no effect on the reaction rate, as it lies hidden behind the highest energy species on the catalytic cycle. In contrast, however, substrates containing alkene substitution demonstrate distinct reaction rates: substituting the alkene methyl group with a phenyl substituent causes an approximately 3-fold decrease in the reaction rate relative to the parent compound. Carboacylation with an extended tether to form a dihydropyran product has a rate constant that is less than 20% that of the parent. This marked difference in reaction rates observed with alkene substitution or extended tether lengths provides clear indication that alkene insertion limits catalyst turnover.

These seemingly contradictory results led to a conclusion that the energy barriers to carbon–carbon bond activation and alkene insertion are quite similar. Utilizing the methyl-substituted alkene present in the parent quinolinyl ketone (1), carbon–carbon bond activation limits catalyst turnover. However, when an alternative alkene with a larger substituent or longer tether is utilized, the sequence of alkene coordination and migratory insertion becomes the highest energy barrier (C to D, Scheme 8). The use of compounds with unfavorable equilibria for alkene coordination and high energy barriers for insertion, such as 1,2-disubstituted alkenes, ultimately results in an insurmountable barrier and product decomposition via various routes.^{32,33}

Catalyst Comparisons. With significant data from extensive mechanistic studies on the carboacylation of alkenes using $\text{RhCl}(\text{PPh}_3)_3$ and $[\text{Rh}(\text{C}_2\text{H}_4)_2\text{Cl}]_2$, we are in a position to evaluate the influence of the catalysts on this reaction with a particular emphasis on the nature of the carbon–carbon bond activation step. Although it is difficult to make direct comparisons due to the different rate laws, under typical reaction conditions, such as with $[\text{I}] = 0.100 \text{ M}$ and 10 mol % rhodium $\{0.010 \text{ M } \text{RhCl}(\text{PPh}_3)_3 \text{ or } 0.005 \text{ M } [\text{Rh}(\text{C}_2\text{H}_4)_2\text{Cl}]_2\}$, the intramolecular alkene carboacylation of quinolinyl ketones proceeds with an initial rate approximately 8 times faster using $[\text{Rh}(\text{C}_2\text{H}_4)_2\text{Cl}]_2$ than using Wilkinson's catalyst.

The primary difference between the two catalyst manifolds is the resting state. Under $\text{RhCl}(\text{PPh}_3)_3$ catalysis, a rhodium–quinoline

complex is proposed as the resting state, leading to an overall first-order rate law that leads to turnover-limiting carbon–carbon bond activation. Due to the complexation at the resting state, the reaction rate demonstrates no dependence on substrate concentration for a majority of the reaction. In contrast, the $[\text{Rh}(\text{C}_2\text{H}_4)_2\text{Cl}]_2$ catalyst resting state is a species uncoordinated to either substrate or product. This species, the exact nature of which remains elusive, must react with the quinolinyl ketone in an associated process prior to turnover-limiting carbon–carbon bond activation, and thus it demonstrates an overall second-order rate law that is dependent on both substrate and catalyst concentrations. The contrasting reaction sequences are also illustrated by the respective activation entropy of each system: the value of $\Delta S^\ddagger = -4.3 \pm 2.4$ eu determined for carboacylation using $\text{RhCl}(\text{PPh}_3)_3$ is consistent with a rearrangement without significant entropic change. In contrast, the value determined under $[\text{Rh}(\text{C}_2\text{H}_4)_2\text{Cl}]_2$ catalysis, $\Delta S^\ddagger = -26.4 \pm 2.6$ eu, indicates an associative process.

Despite the differences in rate laws and resting states, both systems show similar behavior with regard to the turnover-limiting step of catalysis. In each case, significant $^{12}\text{C}/^{13}\text{C}$ kinetic isotope effects are observed on the ketone (an average of 1.027 for $\text{RhCl}(\text{PPh}_3)_3$ and 1.012 for $[\text{Rh}(\text{C}_2\text{H}_4)_2\text{Cl}]_2$) and the adjacent carbon on the aromatic ring (1.026 and 1.015, respectively), indicating that the cleavage of this carbon–carbon bond is the slow step of the reaction.³⁴ In these determinations, the kinetic isotope effects determined for the alkene carbons were within error of 1.000 in all trials with both catalysts, suggesting that this functionality does not play a role in the turnover-limiting step.

The reactivity of the two catalysts diverges somewhat when the reaction is performed with more sterically demanding alkenes or species with longer tether lengths. As the change in alkene is anticipated to have little or no effect on the complexation or carbon–carbon bond activation steps of the catalytic cycle, changes in the observed reaction rates are attributed to the increase in the barrier to alkene migratory insertion. Using $\text{RhCl}(\text{PPh}_3)_3$, this increase in the activation energy of alkene insertion is sufficient to represent an insurmountable barrier, and starting materials, or decomposition products, are recovered. It is hypothesized that the sterically demanding phosphine ligands, of which at least one is anticipated to remain attached to the metal center, provide a very strict limitation on the size of alkene that can coordinate and react.

Under $[\text{Rh}(\text{C}_2\text{H}_4)_2\text{Cl}]_2$ catalysis, a similar but more modest increase in the barrier to alkene migratory insertion is observed. For additional 1,1-disubstituted alkenes or those with longer tether lengths, the barrier is increased sufficiently to make alkene insertion slower than carbon–carbon bond activation, but not to a sufficient extent to preclude the overall transformation.

These results suggest that carbon–carbon bond activation and alkene migratory insertion are quite similar in energy and are susceptible to small changes in the substrate electronic and steric effects. Using $[\text{Rh}(\text{C}_2\text{H}_4)_2\text{Cl}]_2$, the fastest reaction of a substituted analogue of parent ketone **1** occurs with diethylamino-substituted compound **9**, with a rate constant of $0.114 \text{ M}^{-1} \text{ s}^{-1}$. As the Hammett correlation does not deviate from linearity, it suggests that carbon–carbon bond activation still limits this transformation, thus providing an upper limit for the activation barrier for alkene migratory insertion for the parent methyl-substituted alkene.

CONCLUSION

This mechanistic investigation has provided detailed information into the nature of the rhodium-catalyzed carboacylation of

alkenes, with particular insight into the nature of the carbon–carbon bond activation step. These two systems, using $\text{RhCl}(\text{PPh}_3)_3$ or $[\text{Rh}(\text{C}_2\text{H}_4)_2\text{Cl}]_2$ catalysts, provide complementary frameworks for studying carbon–carbon bond activation or alkene migratory insertion steps while also providing a template through which to expand potential reactivity through the interception of reaction intermediates. Efforts are underway to examine the intersection of these two catalyst systems by using the addition of exogenous ligands to $[\text{Rh}(\text{C}_2\text{H}_4)_2\text{Cl}]_2$ in the effort to develop optimized conditions that may be amenable to more expanded reaction scope. Future efforts will be guided by the results of this study, which suggest the use of more electron-rich substrates for the acceleration of carbon–carbon bond activation and the need to focus on alkene insertion as a means of generalizing the carboacylation methodology.

ASSOCIATED CONTENT

Supporting Information

Experimental procedures, kinetic data, characterization information, and spectra. This material is available free of charge via the Internet at <http://pubs.acs.org>.

AUTHOR INFORMATION

Corresponding Author

jjohnson@hope.edu

ACKNOWLEDGMENTS

We thank the Camille and Henry Dreyfus Foundation, the Research Corporation (7833), and the ACS Petroleum Research Fund (50347-UN11) for funding. J.B.J. also thanks the Towsley Foundation for support. We also gratefully acknowledge funding for instrumentation from the NSF (CHE-0922623).

REFERENCES

- (1) de Meijere, A.; Diederich, F. *Metal-catalyzed Cross-Coupling Reactions*, 2nd ed.; Wiley-VCH: Weinheim, 2004.
- (2) (a) Murakami, M.; Ito, Y. In *Activation of Unreactive Bonds and Organic Synthesis*; Murai, S., Ed.; Springer: Berlin, 1999; p 97. (b) Crabtree, R. H. *Chem. Rev.* **1985**, *85*, 245. (c) Jones, W. D. *Nature* **1993**, *364*, 676.
- (3) For leading references, see: (a) Schnuerch, M.; Dastbaravardeh, N.; Ghobrial, M.; Mrozek, B.; Mihovilovic, M. D. *Curr. Org. Chem.* **2011**, *15*, 2694. (b) Jazzar, R.; Hitce, J.; Renaudat, A.; Sofack-Kreutzer, J.; Baudoin, O. *Chem.—Eur. J.* **2010**, *16*, 2654. (c) Giri, R.; Shi, B.-F.; Engle, K. M.; Mauge, N.; Yu, J.-Q. *Chem. Soc. Rev.* **2009**, *38*, 3242. (d) Chen, X.; Engle, K. M.; Wang, D.-H.; Yu, J.-Q. *Angew. Chem., Int. Ed.* **2009**, *48*, 5094. (e) Crabtree, R. H. *Dalton Trans.* **2001**, 2437. (f) Crabtree, R. H. *J. Chem. Soc., Dalton Trans.* **2001**, 2437. (g) Dyker, G. *Angew. Chem., Int. Ed.* **1999**, *38*, 1699. (h) Arndtsen, B. A.; Bergman, R. G.; Mobley, T. A.; Peterson, T. H. *Acc. Chem. Res.* **1995**, *28*, 154.
- (4) For leading references, see: (a) Murakami, M.; Matsuda, T. *Chem. Commun.* **2011**, 47, 1100. (b) Nečas, D.; Kotora, M. *Curr. Org. Chem.* **2007**, *11*, 1566. (c) Murakami, M.; Makino, M.; Ashida, S.; Matsuda, T. *Bull. Chem. Soc. Jpn.* **2006**, *79*, 1315. (d) Jun, C.-H. *Chem. Soc. Rev.* **2004**, *33*, 610.
- (5) Significant advances have been made in the activation of C–CN bonds. For leading references, see: (a) Hirata, Y.; Yada, A.; Morita, E.; Nakao, Y.; Hiyama, T.; Ohashi, M.; Ogoshi, S. *J. Am. Chem. Soc.* **2010**, *132*, 10070. (b) Nakao, Y.; Yada, A.; Hiyama, T. *J. Am. Chem. Soc.* **2010**, *130*, 10024. (c) Najara, C.; Sansano, J. M. *Angew. Chem., Int. Ed.* **2009**, *48*, 2452. (d) Nakao, T.; Ebata, S.; Yada, A.; Hiyama, T.; Ikawa, M.; Ogoshi, S. *J. Am. Chem. Soc.* **2008**, *130*, 12874. (e) Watson, M. P.; Jacobsen, E. N. *J. Am. Chem. Soc.* **2008**, *130*, 12594. (f) Ysaui, Y.;

Kamisaki, H.; Takemoto, Y. *Org. Lett.* **2008**, *10*, 3303. (g) Tobisu, M.; Kita, Y.; Ano, Y.; Chantani, N. *J. Am. Chem. Soc.* **2008**, *130*, 15982. (h) Nishihara, Y.; Inoue, Y.; Itazaki, M.; Takagi, K. *Org. Lett.* **2005**, *7*, 2639. (i) Penney, J. M.; Miller, J. M. *Tetrahedron Lett.* **2004**, *45*, 4989.

(6) Some success has been achieved with strategies such as retro-aldol and retro-allylation sequences. See refs 7 and 8. For retro-Claisen reactions, see: (a) Grenning, A. J.; Tunge, J. A. *J. Am. Chem. Soc.* **2011**, *133*, 14785. (b) Han, C.; Kim, E. H.; Colby, D. A. *J. Am. Chem. Soc.* **2011**, *133*, 5802. (c) Deb, I.; Seidel, D. *Tetrahedron Lett.* **2010**, *51*, 2945. (d) Biswas, S.; Maiti, S.; Jana, U. *Eur. J. Org. Chem.* **2010**, 2861. (e) He, C.; Guo, S.; Huang, L.; Lei, A. *J. Am. Chem. Soc.* **2010**, *132*, 8273. (f) Wei, Y.; Lui, J.; Lin, S.; Ding, H.; Liang, F.; Zhao, B. *Org. Lett.* **2010**, *12*, 4220.

(7) Kuninobu, Y.; Kawata, A.; Takai, K. *J. Am. Chem. Soc.* **2006**, *128*, 11368.

(8) For retro-allylation, see: (a) Yorimitsu, H.; Oshima, K. *Bull. Chem. Soc. Jpn.* **2009**, *82*, 778. (b) Turský, M.; Nečas, D.; Drabina, P.; Sedláč, M.; Katora, M. *Organometallics* **2006**, *25*, 901. (c) Nilsson, Y. I. M.; Andersson, P. G.; Bäckvall, J.-E. *J. Am. Chem. Soc.* **1993**, *115*, 6609. (d) Nečas, D.; Turský, M.; Katora, M. *J. Am. Chem. Soc.* **2004**, *126*, 10222. (e) Kondo, T.; Kodoi, K.; Nishinaga, E.; Okada, T.; Morisaki, Y.; Watanabe, Y.; Mitsudo, T.-a. *J. Am. Chem. Soc.* **1998**, *120*, 5587. (f) Oh, C. H.; Jung, S. H.; Bang, S. Y.; Park, D. I. *Org. Lett.* **2002**, *4*, 3325. (g) Takada, Y.; Hayashi, S.; Hirano, K.; Yorimitsu, H.; Oshima, K. *Org. Lett.* **2006**, *8*, 2515.

(9) For leading references, see: (a) Satoh, T.; Jones, W. D. *Organometallics* **2001**, *20*, 2916. (b) Müller, C.; Lachicotte, R. J.; Jones, W. D. *Organometallics* **2002**, *21*, 1975. (c) Kondo, T.; Kaneko, Y.; Taguchi, Y.; Nakamura, A.; Okada, T.; Shiotsuki, M.; Ura, Y.; Wada, K.; Misudo, T. *J. Am. Chem. Soc.* **2002**, *124*, 6824. (d) Ashida, S.; Murakami, M. *Bull. Chem. Soc. Jpn.* **2008**, *81*, 885.

(10) For leading references, see: (a) Jun, C.-H.; Moon, C. W.; Lee, D.-Y. *Chem.—Eur. J.* **2002**, *8*, 2422. (b) Park, Y. J.; Park, J.-W.; Jun, C.-H. *Acc. Chem. Res.* **2008**, *41*, 222.

(11) (a) Salem, H.; Ben-David, Y.; Shimon, L. J. W.; Milstein, D. *Organometallics* **2006**, *25*, 2292. (b) Rybtchinski, B.; Milstein, D. *Angew. Chem., Int. Ed.* **1999**, *38*, 870 and references therein.

(12) (a) Seiser, T.; Cramer, N. *J. Am. Chem. Soc.* **2010**, *132*, 5340. (b) Matsuda, T.; Shigeno, M.; Makino, M.; Murakami, M. *Org. Lett.* **2006**, *8*, 3379.

(13) (a) Terao, Y.; Wakui, H.; Satoh, T.; Miura, M.; Nomura, M. *J. Am. Chem. Soc.* **2001**, *123*, 10407. (b) Terao, Y.; Wakui, H.; Nomoto, M.; Satoh, T.; Miura, M.; Nomura, M. *J. Org. Chem.* **2003**, *68*, 5236. (c) Terao, Y.; Nomoto, M.; Satoh, T.; Miura, M.; Nomura, M. *J. Org. Chem.* **2004**, *69*, 6942.

(14) Matsumura, S.; Maeda, Y.; Nishimura, T.; Uemura, S. *J. Am. Chem. Soc.* **2003**, *125*, 8862.

(15) (a) Seiser, T.; Roth, O. A.; Cramer, N. *Angew. Chem., Int. Ed.* **2009**, *48*, 6320. (b) Shigeno, M.; Yamamoto, T.; Murakami, M. *Chem.—Eur. J.* **2009**, *15*, 12929.

(16) For an example of C—C activation coupled with N₂ extrusion, see: Chiba, S.; Xu, Y.-J.; Wang, Y.-F. *J. Am. Chem. Soc.* **2009**, *131*, 12886.

(17) Li, H.; Li, Y.; Zhang, X.-S.; Chen, K.; Wang, X.; Shi, Z.-J. *J. Am. Chem. Soc.* **2011**, *133*, 15244.

(18) Nishimura, T.; Katoh, T.; Takatsu, K.; Shintani, R.; Hayashi, T. *J. Am. Chem. Soc.* **2007**, *129*, 14158.

(19) For reactions with alkynes, see: Schaub, T.; Backes, M.; Radius, U. *Organometallics* **2006**, *25*, 4196.

(20) (a) Dreis, A. M.; Douglas, C. J. *J. Am. Chem. Soc.* **2009**, *131*, 412. (b) Wentzel, M. T.; Reddy, V. J.; Hyster, T. K.; Douglas, C. J. *Angew. Chem., Int. Ed.* **2009**, *48*, 6121.

(21) (a) Iverson, C. N.; Jones, W. D. *Organometallics* **2001**, *20*, 5745. (b) Murakami, M.; Itahashi, T.; Ito, Y. *J. Am. Chem. Soc.* **2002**, *124*, 13976. (c) Wender, P. A.; Correa, A. G.; Sator, Y.; Sun, R. *J. Am. Chem. Soc.* **2000**, *122*, 7815. (d) Yamamoto, Y.; Kuwabara, S.; Hayashi, H.; Nishiyama, H. *Adv. Synth. Catal.* **2006**, *348*, 2493. (e) Crépin, D.; Dawick, J.; Aissa, C. *Angew. Chem., Int. Ed.* **2010**, *49*, 620.

(22) For examples of enantioselective C—C activation, see: (a) Nishimura, T.; Matsumura, S.; Maeda, Y.; Uemura, S. *Chem. Commun.* **2002**, 50. (b) Matsuda, T.; Shigeno, M.; Makino, M.; Murakami, M. *Org. Lett.* **2006**, *8*, 3379. (c) Matsuda, T.; Shigeno, M.; Murakami, M. *J. Am. Chem. Soc.* **2007**, *129*, 12086. (d) Sieser, T.; Cramer, N. *Angew. Chem., Int. Ed.* **2006**, *45*, 3957. (e) Trost, B. M.; Zie, J. *J. Am. Chem. Soc.* **2008**, *130*, 6231 and ref 5e.

(23) Rathbun, C. M.; Johnson, J. B. *J. Am. Chem. Soc.* **2011**, *133*, 2031.

(24) (a) Ateşin, T. A.; Li, T.; Lachaize, S.; García, J. J.; Jones, W. D. *Organometallics* **2008**, *27*, 3811. (b) Li, T.; García, J. J.; Brennessel, W. W.; Jones, W. D. *Organometallics* **2010**, *29*, 2430. (c) Evans, M. E.; Li, T.; Jones, W. D. *J. Am. Chem. Soc.* **2010**, *132*, 16278.

(25) For related mechanistic studies on stoichiometric systems, see: (a) Obenhuber, A.; Ruhland, K. *Organometallics* **2011**, *30*, 4039. (b) Suggs, J. W.; Jun, C.-H. *J. Am. Chem. Soc.* **1984**, *106*, 3054. (c) Suggs, J. W.; Jun, C.-H. *J. Am. Chem. Soc.* **1986**, *108*, 4679.

(26) (a) Singleton, D. A.; Thomas, A. A. *J. Am. Chem. Soc.* **1995**, *117*, 9357. (b) Frantz, D. E.; Singleton, D. A.; Snyder, J. P. *J. Am. Chem. Soc.* **1997**, *119*, 3383.

(27) See the Supporting Information for full kinetic results and experimental methods.

(28) Hansch, C.; Leo, A. *Substituent Constants for Correlation Analysis in Chemistry and Biology*; Wiley-Interscience: New York, 1979.

(29) See the Supporting Information for complete results, analysis methods, and the experimental methods.

(30) For leading references, see: (a) Brown, J. M.; Cooley, N. A. *Chem. Rev.* **1988**, *88*, 1031. For discussion within a catalytic cycle, see: (b) Espinet, P.; Echavarren, A. M. *Angew. Chem., Int. Ed.* **2004**, *43*, 4704. (c) Denmark, S. E.; Sweis, R. F. *J. Am. Chem. Soc.* **2004**, *126*, 4876. (d) Jones, G. D.; Martin, J. L.; McFarland, C.; Allen, O. R.; Hall, R. E.; Haley, A. D.; Brandon, R. J.; Konovalova, T.; Desrochers, P. J.; Pulay, P.; Vivic, D. A. *J. Am. Chem. Soc.* **2006**, *128*, 13175.

(31) For exceptions, see: (a) Johnson, J. B.; Bercot, E. A.; Rowley, J. M.; Coates, G. W.; Rovis, T. *J. Am. Chem. Soc.* **2007**, *129*, 2718. (b) Pfretschner, T.; Kleeman, L.; Janza, B.; Harms, K.; Schrader, T. *Chem.—Eur. J.* **2004**, *10*, 6048. Other systems with rate-limiting reductive elimination: (c) C—H bond formation: Halpern, J. *Asymmetric Synthesis*; Academic Press: New York, 1983; Vol 5, p 48. (d) C—S bond formation: Moreau, X.; Campagne, J. M.; Meyer, G.; Jutand, A. *Eur. J. Org. Chem.* **2005**, 3749.

(32) Hanley, P. S.; Hartwig, J. F. *J. Am. Chem. Soc.* **2011**, *133*, 15661.

(33) Johnson, J. B.; Rovis, T. *Angew. Chem., Int. Ed.* **2008**, *47*, 840.

(34) For additional examples of the use of ¹²C/¹³C kinetic isotope effects in mechanistic studies, see: (a) Gómex-Gallego, M.; Sierra, M. A. *Chem. Rev.* **2011**, *111*, 4857. (b) Yoshikai, N.; Matsuda, H.; Nakamura, E. *J. Am. Chem. Soc.* **2008**, *130*, 15258. (c) Denmark, S. E.; Bui, T. *J. Org. Chem.* **2005**, *70*, 10393. (d) Švenda, J.; Evans, A. G. *Org. Lett.* **2009**, *11*, 2437. (e) Edwards, D. R.; Montoya-Peleaz, C.; Cruden, C. M. *Org. Lett.* **2007**, *9*, 5481.